2020 IEEE PELS Workshop on Emerging Technologies: Wireless Power Transfer (WoW)

November 15 - 19, 2020, Seoul, Korea

An Electrodynamic Wireless Power Receiver 'Chip' for Wearables and Bio-implants

Miah A. Halim, Adrian A. Rendon-Hernandez, David P. Arnold*
Interdisciplinary Microsystems Group, Dept. of Electrical and Computer Engineering
University of Florida, Gainesville, Florida 32611, USA
*darnold@ufl.edu

***Abstract*—This paper presents the design, fabrication and experimental characterization of a chip-sized wireless power receiver for low-frequency electrodynamic wireless power transmission (EWPT). Utilizing a laser micro-machined meandering suspension, one NdFeB magnet, and two PZT-5A piezoelectric patches, this 0.08 cm^3 micro-receiver operates at its torsion mode mechanical resonance of 724 Hz. The device generates 360 µW average power (4.2 mWcm^{-3} power density) at 1 cm distance from a transmitter coil operating at 724 Hz and safely within allowable human exposure limits of 2 mT$_{rms}$ field. Compared to a previously reported macro-scale prototype, this volume-efficient micro-receiver is 31x smaller and offers 3.2x higher power density within a low-profile, compact footprint for wirelessly charging wearable and bio-implantable devices.**

Keywords*— *electrodynamic coupling, electromechanical devices, micro-assembly, meandering suspension, piezoelectric transducers, wireless power

I. Introduction

Now-a-days, traditional power supply cords have become less important due to their limitations in large-scale utilization and mobility. Additionally, the use of portable power sources (i.e., batteries) as a substitute to power cords is not an optimal solution as batteries have a short lifetime. Recharging or replacing batteries is impractical and incurs operational costs. Wireless power transmission (WPT) technologies allow electromagnetic wave energy to be transferred from a power source (transmitters) to destinations (receivers) wirelessly. They provide a deterministic method for actively transferring power to electronic devices while removing the burden of plugging in a charging cable. Recent progress in WPT techniques motivate new avenues of research in different applications e.g., portable electronic devices, electric vehicles, medical implants, Internet of Things (IoT) sensors, unmanned aerial vehicles, and so on. Near-field electromagnetic energy transfer approaches such as inductive, magnetic resonance or capacitive coupling between transmitter and receiver are commonly used in such applications [1].

To date, most research has been focused on inductively coupled WPT in which a transmitter coil produces a time-varying magnetic field that directly induces a voltage in a receiver coil at remote distance. It is well suited for efficient (>80 %) power transmission over a distance much smaller than the coil diameter, but its performance decreases dramatically when the distance between the transmitter and receiver increases [2]. Magnetic resonance WPT is a specialized case of inductive WPT wherein electrical resonance is used in the transmitter and receiver that increases both efficiency and transmission distance over several coil diameters [3]. The operating frequency of these WPT techniques is typically in the range of MHz, which generates unwanted eddy currents (also called Foucault currents) in the case when the receiver is blocked by electrically conductive objects. These eddy currents flow in closed loops within an object, in planes perpendicular to the applied magnetic field [4]. As a result, the eddy currents can attenuate or alter the fields used for power transmission and can cause undesirable heating in the intervening objects. In order to address these constraints, particularly for wearable and implantable medical devices, much lower frequencies have been considered using an electrodynamically coupled approach between a transmitter and a permanent magnet in a receiver [5].

An electrodynamic WPT (EWPT) system utilizes a permanent magnet in the receiver that oscillates when subjected to a time-varying magnetic field supplied from a transmitter. The vibration of the magnet is then converted into electricity by one or more electromechanical transduction schemes (e.g. electromagnetic induction, piezoelectric, or capacitive). The main advantage of the EWPT method is that it operates at much lower frequencies (<1 kHz) than that of the conventional inductively coupled systems (0.1–10 MHz) that allows higher magnetic fields for safe exposure to human. IEEE standards set the maximum allowable human exposure limit for head/torso in controlled environment at 1 MHz is ~0.6 mT whereas it is 2 mT at 1 kHz which is over 3x larger [6,7]. This low-frequency operation conceals the field attenuation and parasitic heating effects while transmitting through conductive media (e.g., metal, human body etc.) [8]. For instance, an EWPT system using a rotating permanent magnet receiver demonstrated simultaneous charging of multiple wearable electronic devices in a cluttered environment [9]. Model validation and analytical investigation of piezoelectric cantilever based EWPT receivers has also been reported [10]. Recently, our group has introduced a piezoceramic EWPT receiver using a meandering suspension using a 2.5 cm^3 prototype [11].

In this paper, we report a low-profile (1.5 mm), low-footprint (7.6 × 7.6 mm^2) EWPT micro-receiver using a laser micro-machined suspension that significantly reduces the volume of the device and increases both the quality factor (Q-factor) and power density while still operating within the maximum allowable magnetic field exposure limits for wearables and bioimplants.

II. EWPT Micro-Receiver Design and Operation

Figure 1 illustrates the schematic structure of the EWPT micro-receiver and its operation principle. It is comprised of a double-clamped meandering suspension with a center platform where a laterally magnetized square permanent magnet is mounted by a spacer. Two piezo-ceramic patches are attached to the clamped arms (on the side opposite to the magnet) to form unimorph transducers in series connection. The external dimensions of the micro-receiver are 7.6 mm × 7.6 mm and only 1.5 mm thick. When subjected to an external time-varying magnetic field, the magnet resonates torsionally and stresses are generated on the piezo-ceramic elements which, in turn, generate voltages by means of the

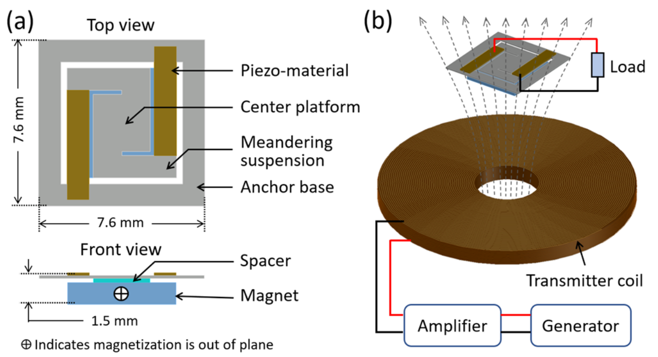

Fig. 1. (a) Schematic structure of the EWPT micro-receiver and (b) its operation principle under time-varying magnetic field transmitted from a transmitter coil.

piezoelectric effect. The time-varying magnetic fields of desired frequency and amplitude are generated by supplying alternating current to a transmitter coil.

The proposed EWPT system using piezoelectric micro-receiver can be represented by an equivalent electrical circuit shown in Fig. 2. The energy from the source is flowing from the electrical domain through the transmitter coil, to the mechanical domain via a spring-mass-damper in the receiver, and then back to the electrical domain through the piezoelectric transducers and a load. Two transductions between the electrical and the mechanical domains are achieved through both electrodynamic Γ_M and piezoelectric Γ_P couplings. An alternating magnetic field $\vec{B}$ produced by the transmitter, induces a torque $\vec{\tau}_{mag}$ on the receiver magnet which is dependent on the relative position and orientation and is given by [5]

$$\tau_{mag} = |\vec{m} \times \vec{B}| = M.v_{mag}.B_0 \qquad (1)$$

where $\vec{m}$ is the magnetic moment, M is the magnetization field, v_{mag} is the magnet volume, and B_0 is the magnetic flux density. When a load resistance R_L is connected, the voltage V_L generated across the load and the amount of power P_{out} delivered to the load can be given as [12]

$$V_L = \frac{\Gamma_P \tau_{mag}}{\left(b + j\omega J + \frac{k}{j\omega}\right)(1 + j\omega C_P R_L) + \Gamma_P^2 R_L} R_L \qquad (2)$$

$$P_{out} = \frac{1}{2} \cdot \frac{V_L^2}{R_L} \qquad (3)$$

where Γ_P is the turn ratio of the electromechanical transformer, b is the mechanical damping coefficient, J is the mass moment of inertia of the magnet, k is the short-circuit stiffness of the meandering suspension, and ω is the angular frequency, and C_p is the equivalent capacitance of the piezoelectric transducers.

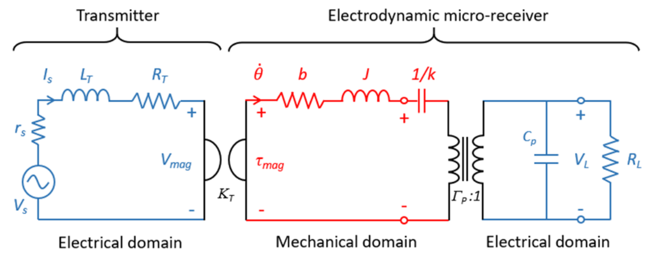

Fig. 2. Equivalent electrical circuit representation of the proposed EWPT system and its energy domain flow.

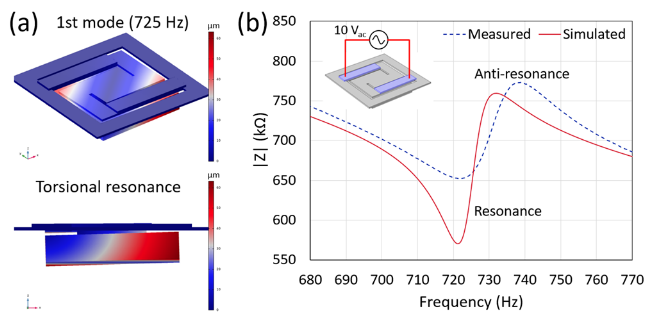

Fig. 3. FEA simulation results: (a) 1st mode torsional resonance and (b) frequency domain study to determine the piezoelectric impedance of the micro-receiver.

The micro-receiver has been designed to operate at its 1st mode torsional resonance (~725 Hz) which was determined by finite element analysis (FEA) simulation using COMSOL MultiPhysics®, as shown in Fig. 3(a). In this situation, the top surface of one piezo-ceramic transducer is in tension and the other is in compression. Therefore, simultaneous voltages generated by each piezo-ceramic transducer are in opposite polarities and are added together when connected in series via the metal anchor base. Then, a frequency domain study was performed to examine the piezoelectric impedance of the system by applying 10V AC supply to the terminals of piezoelectric elements as illustrated in Fig. 3(b). A damping (ζ) loss of 1.25% (estimated from measured Q-factor, $Q = 1/2\zeta$) and a dielectric loss factor ($\tan\delta$) of 0.02 (obtained from material datasheet) were considered in the FEA simulation. Note that, a 20 µm thick uniform adhesive layer was considered in the model as well. Figure 3(b) shows the piezoelectric impedance values around the first resonance mode for both simulation and measurement. However, other losses (e.g., viscous damping) were not considered in the simulation that lead to the variation with the measurement. Current efforts on exploring electromechanical modeling are ongoing in order to predict its performances accurately and to facilitate optimizing the system.

III. Protype Fabrication and Characterization

A micro-receiver prototype was fabricated to test under various magnetic fields with resistive loads. Figure 4 shows the schematics of the fabrication and assembly process and the photographs after each process step. The meandering beam structure was formed by laser micro-machining 125 µm thick titanium (Ti) shim stock. The width of the meandered beam was 1 mm and the area of the center

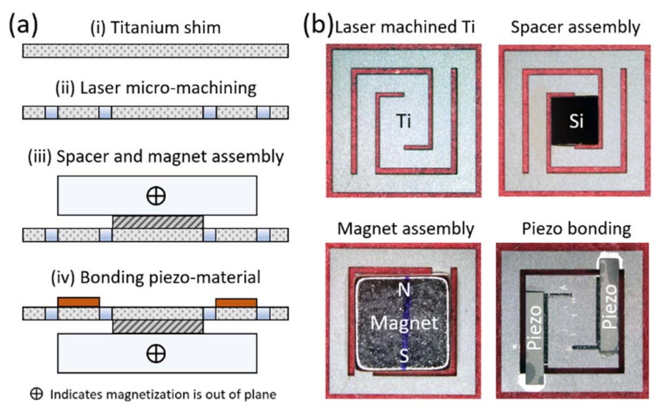

Fig. 4. (a) Schematics and (b) photographs of the fabrication and assembly process of the EWPT micro-receiver.

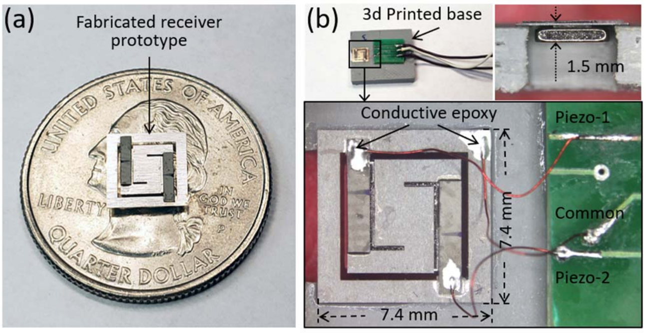

Fig. 5. Photographs of the (a) fabricated prototype with size compared to a US quarter dollar and (b) ready to test, fully assembled prototype.

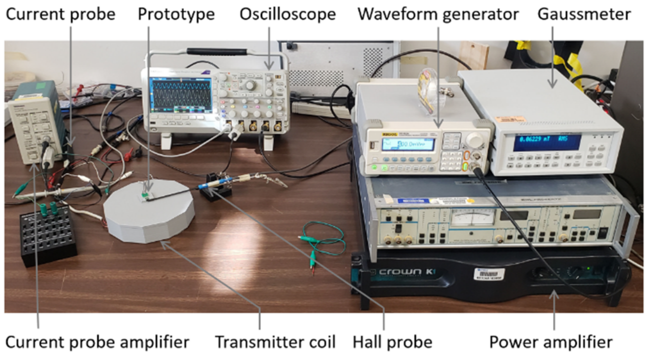

Fig. 6. Photograph of the experimental characterization of the fabricated EWPT micro-receiver prototype.

platform was 2.6×2.6 mm^2. A same sized silicon (Si) spacer, diced out of a 200-µm-thick Si wafer and a laterally magnetized N50 NdFeB magnet (5×5×1 mm^3) were bonded using cyanoacrylate to one side of the center platform. On the opposite side, two piezo-ceramic patches (5×1×0.13 mm^3), diced from a large PZT-5A sheet with sputtered Nickel electrodes, poled through thickness (Piezo Systems, USA), were bonded to the clamped arms of the meandered beam using electrically conductive silver epoxy (EO-21M-5, EpoxySet Inc., USA) to form a series electrical connection between the transducers. Finally, the entire structure was clamped to a 3D printed plastic base and electrical connections (for measurements) were created by bonding thin copper wires using silver epoxy, as shown in Fig. 5b.

The fully assembled micro-receiver prototype was tested under various alternating magnetic fields transmitted from a single pancake type transmitter coil. Figure 6 shows a photograph of the experimental setup. The micro-receiver prototype was placed on the top surface of the plastic box (at the center) containing the transmitter coil and a 2 cm axial distance was maintained between the face of the receiver magnet and the surface of the coil. The coil used here (Ø150 mm × 15 mm) is made of 169 turns of 12 AWG copper magnet wire. It generates uniaxial fields and has a coil figure-of-merit (f_m) of 13.4×10^6 W.T^{-2} [8]. An arbitrary waveform generator (Rigol DG1022A) was used to supply an AC voltage to a power amplifier (Crown K1) that produced an alternating current input into the transmitter coil, monitored by a current probe (Tektronix TCP312A) connected to a current probe amplifier (Tektronix TCPA300). An oscilloscope (Tektronix DPO-2004B) was used to measure the input current to the transmitter coil , as well as the output voltage generated by the micro-receiver. For a given AC excitation of the transmitter coil, the resultant B field spatial distribution was measured with a

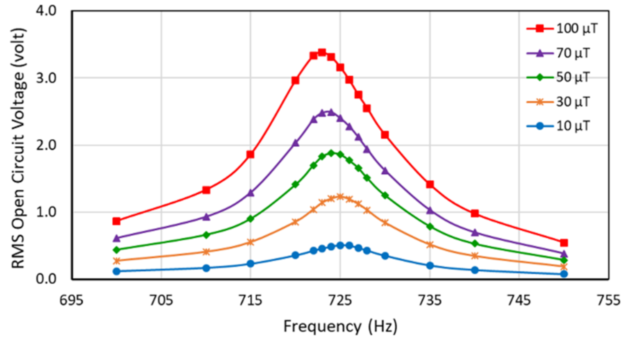

Fig. 7. Measured open circuit voltage as a function of frequency for various magnetic fields transmitted from the coil at 2 cm axial distance.

Hall probe (Lakeshore HMNT- 4E04 -VR) connected to a gaussmeter (Lakeshore 475DSP).

IV. Results and Discussion

First, we determined the 1st mode torsional resonance of the micro-receiver by measuring the open circuit root mean square (rms) voltage as a function of operating frequency of the magnetic fields with various amplitudes (between 10 and 100 µT$_{rms}$), as shown in Fig. 7. As seen from the figure, the micro-receiver exhibits a fairly linear characteristic at its resonance (~724 Hz) that indicates an underdamped 2nd-order system with Q-factor up to 75 in the air. There is a slight difference between the FEA modal simulation and the experimental results that is attributed due to the process variation in assembling the micro-receiver components and uneven bond layer between the Ti base and piezo-ceramic patches, which were not considered in the FEA simulation.

Figure 8 shows the measured rms voltage and time-average power delivered to continually adjustable load resistances (varied from 50 to 4000 kΩ) while using a constant amplitude, 100 µT$_{rms}$ alternating magnetic field at 724 Hz resonance. The time-average power was calculated by using V_{rms}^2/R_l , where V_{rms} is the rms value of the measured voltage across each load resistance R_l . Results show that the rms voltage increases with the increase in the resistance value, however, a maximum power (13 µW) was obtained with an optimum load resistance of 650 kΩ. Next, the amplitude of the alternating magnetic field was varied, while the frequency was kept constant at 724 Hz and using the previously determined optimal load resistance. Figure 9 shows that the voltage increases ~linearly up to 200 µT$_{rms}$, but some nonlinearity is observed beyond that. The time-average power delivered to the load correspondingly increases with the magnetic field that reaches up to 130 µW for 500 µT$_{rms}$ magnetic field.

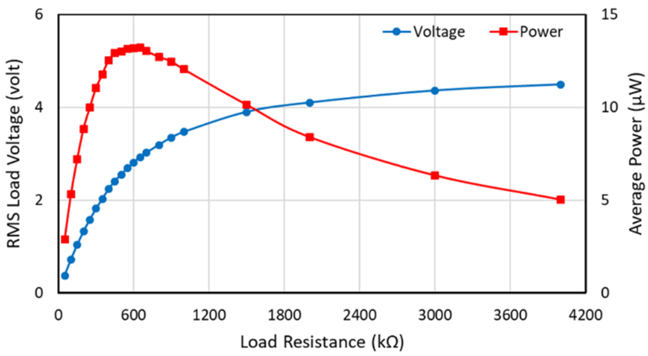

Fig. 8. Measured voltage and power vs. load resistance under 100 µT$_{rms}$ magnetic field at 724 Hz resonant frequency.

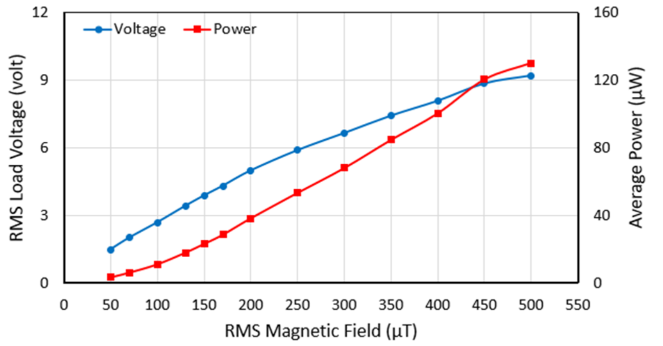

Fig. 9. Measured power (and voltage) delivered to 650 kΩ optimum load under various magnetic fields at 724 Hz resonant frequency.

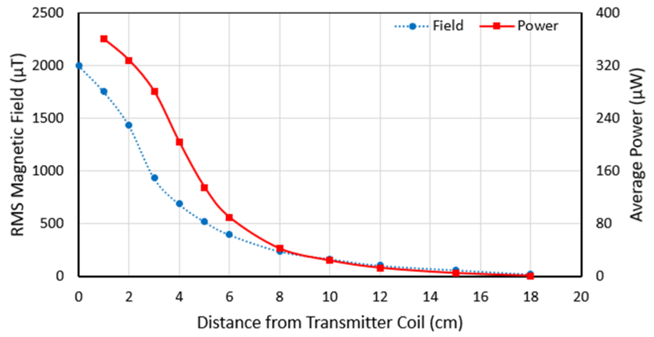

Fig. 10. Measured power and magnetic field vs. axial distance between the transmitter coil and micro-receiver prototype while a maximum allowable safe field of 2 mT_{rms} at 724 Hz was generated at the center of the coil.

Finally, the time-average power was measured as a function of distance (up to 18 cm) between the transmitter coil and the micro-receiver prototype, as shown in Fig. 10. In this case, a maximum of 2 mT_{rms} field at 724 Hz frequency (within human exposure safety limit) was generated at the center (right on the surface) of the transmitter coil by limiting the current to the coil at 979 mA_{rms}. It is obvious that the field amplitude at the micro-receiver location decays as distance increases. As seen from the figure, the prototype generated a maximum of 360 µW power at a distance of 1 cm from the transmitter coil, that corresponds to 4.2 $mWcm^{-3}$ power density. The power generation certainly decreases as the magnetic field weakens as the distance from the source increases. However, the micro-receiver prototype was still able to generate meaningful power (24 µW) at 10 cm distance where the magnetic field strength was measured as 161 μT_{rms}.

V. Conclusion

In this work, we have successfully designed, fabricated and tested a laser micro-machined, low-profile EWPT micro-receiver using two simultaneously operating piezo-ceramic transducers on a torsionally resonated meandering suspension for near-field WPT, well suited for wearable and implantable biomedical applications. An equivalent electromechanical model has been established and experimentally demonstrated its performances. Experimental results reveal that the 0.08 cm^3 prototype generated maximum 360 µW average power at 724 Hz frequency at an axial near-field distance of 1 cm from a transmitter coil operating within IEEE safety standards for human exposure limit of 2 mT_{rms}. As compared to a previously reported macro prototype [11], this volume-efficient micro-prototype is 31x smaller, offers ~2x higher Q-factor, 3.2x larger power density, and 1.4x higher NPD operating at the same distance (10 cm) from the transmitter coil.

Acknowledgment

This work was supported in part by the NSF I/UCRC on Multi-functional Integrated System Technology (MIST) Center (NSF Grant IIP-1439644).

References

[1] A. M. Jawad, R. Nordin, S. K. Gharghan, H. M. Jawad, and M. Ismail, "Opportunities and challenges for near-field wireless power transfer: a review", Energies, vol. 10, p. 1022, July 2017.

[2] D. Kim, A. Abu-Siada, and A. Sutinjo, "State-of-the-art literature review of WPT: Current limitations and solutions on IPT", Electr. Pow. Syst. Res., vol. 154, pp. 493– 502, September 2017.

[3] S. D. Barman, A. W. Reza, N. Kumar, M. E. Karim, and A. B. Munir, "Wireless powering by magnetic resonant coupling: recent trends in wireless power transfer system and its applications", Renew. Sustain. Energy Rev., vol. 51, pp. 1525– 1552, July 2015.

[4] Y. Ding-Xin, H. Zheng, Z. Hong, H. Hai-Feng, S. Yun-Zhe, and H. Bao-Jian, "Through-metal-wall power delivery and data transmission for enclosed sensors: a review", Sensors, vol. 15, pp. 31581– 31605, December 2015.

[5] V. R. Challa, J. O. Mur-Miranda, and D. P. Arnold, "Wireless power transmission to an electromechanical receiver using low-frequency magnetic fields," Smart Mater. Struct., vol. 21, p. 115017, October 2012.

[6] IEEE, "Standard for safety levels with respect to human exposure to radio frequency electromagnetic fields, 3 kHz to 300 GHz", IEEE Std. C95.1-2010, pp. 1– 238, March 2010.

[7] IEEE, "Standard for Ssfety levels with respect to human exposure to electromagnetic fields, 0-3 kHz", IEEE Std. C95.6-2002, pp. 1– 43, October 2002.

[8] N. Garraud, D. Alabi, S. Chyczewski, J. D. Varela, D. P. Arnold, and A. Garraud, "Extending the range of wireless power transmission for bioimplants and wearables", J. Phys: Conf. Series, vol. 1052, p. 012023, July 2018.

[9] N. Garraud, A. Garraud, D. Munzer, M. Althar, and D. P. Arnold, "Modeling and Experimental Analysis of Rotating Magnet Receivers for Electrodynamic Wireless Power Transmission", J. Phys. D: Appl. Phys., vol. 52, p.185501, February 2019.

[10] B. D. Truong, S. Williams, and S. Roundy, "Experimentally validated model and analytical investigations on power optimization for piezoelectric-based wireless power transfer systems", J. Intel. Mat. Syst. Str., vol. 30, pp. 2464– 2477, July 2019.

[11] M. A. Halim, J. M. Samman, S. E. Smith, and D. P. Arnold, "Piezoceramic electrodynamic wireless power receiver using torsion mode meandering suspension" PowerMEMS 2019, Krakow, Poland, 2-6 December, 2019.

[12] G. Liu, P. Ci, and S. Dong, "Energy harvesting from ambient low-frequency magnetic field using magneto-mechano-electric composite cantilever", Appl. Phys. Lett., vol. 104, p. 032908, January 2014.